Check for updates

Structural and functional characterization of the mouse von Willebrand factor receptor GPIb-IX with novel monoclonal antibodies

Wolfgang Bergmeier, Kirsten Rackebrandt, Werner Schröder, Hubert Zirngibl, and Bernhard Nieswandt

Five novel monoclonal antibodies (mAbs; p0p 1-5) were used to characterize the structural and functional properties and the in vivo expression of the murine GPIb-IX complex (von Willebrand factor receptor). The molecular weights of the subunits are similar to the human homologs: GPIbα (150 kd), GPIbβ (25 kd), and GPIX (25 kd). Activation of platelets with thrombin or PMA predominantly induced shedding of glycocalicin (GC; 130 kd) but only low levels of receptor internalization. The GC concentration in normal mouse plasma was found to be at least 10 times higher than that described for human plasma (approximately 25 μg/mL versus 1-2 μg/mL). Two additional cleavage sites for unidentified platelet-derived proteases were found on GPIbα, as demonstrated by the generation of 3 N-terminal fragments during in vitro incubation of washed platelets (GC, 60 kd, 45 kd). Occupancy of GPIbα with p0p mAbs or F(ab)$_2$-fragments resulted in aggregate formation in vitro and rapid irreversible thrombocytopenia in vivo, irrespective of the exact binding epitopes of the individual antibodies. GPIb-IX was not detectable immunohistochemically on endothelial cells in the major organs under normal or inflammatory conditions. The authors conclude that the mouse system might become an interesting model for studies on GPIb-IX function and regulation. (Blood. 2000;95:886-893)

© 2000 by The American Society of Hematology

Introduction

Platelet adhesion to sites of vascular injuries is mediated by the interactions of glycoprotein (GP) membrane receptors on circulating platelets with their distinct adhesive ligands.[1] In particular, under high shear stress, the platelet GPIb-IX-V receptor complex contributes to this process initiating hemostasis through interactions with the adhesive ligand von Willebrand factor (vWF).[2-4] The human GPIb-IX-V complex consists of 4 distinct gene products: GPIbα, Ibβ, IX, and V.[5,6] Unstimulated platelets express approximately 25 000 copies of GPIb-IX and 12 000 copies of GPV on their surfaces.[6] Binding sites for vWF and α-thrombin have been identified on the N-terminal 45-kd region of GPIbα.[7-9] Interactions with vWF molecules only occur when the latter are bound to subendothelium,[10] fibrin,[11] or collagen,[12] and they require high shear forces.[13] Interactions are also detectable during ristocetin- or botrocetin-induced platelet agglutination, probably because of neutralization of the repulsive negative charges by the positively charged ristocetin or botrocetin molecules.[14-16] Subsequent activation of the fibrinogen receptor GPIIbIIIa leads to the formation of stronger bonds and therefore platelet adhesion and aggregation.[4,17] In contrast, other platelet agonists such as adenosine diphosphate, collagen, or thrombin induce the binding of vWF to GPIIbIIIa.[18,19] The effect of platelet activation on the surface expression of GPIb-IX in vitro has been a matter of controversy. Although most investigators demonstrate the translocation of GPIb-IX–complexes from the plasma membrane to the surface-connected canalicular system in response to thrombin (without receptor shedding),[20-22] significant shedding has been observed by others.[23] Furthermore, White et al[24] found no effect of thrombin activation on GPIb-IX surface expression. In contrast, it is commonly accepted that GPIbα can be proteolyzed by neutrophil cathepsin G,[25] neutrophil elastase,[26] or platelet calpain.[27]

The platelets of patients with Bernard-Soulier syndrome, a congenital bleeding disorder, show diminished agglutination to vWF in the presence of ristocetin and a reduced response to low doses of thrombin. This results from a reduced expression or a malfunction of GPIb-IX[28] that coincides with the release of ''giant'' platelets,[1,2] indicating a role of the GPIb-IX-V complex in maintaining circulating platelet morphology. Reports describing the expression of GPIbα or even all subunits of the receptor complex on cells of nonhematopoietic origin, particularly endothelial cells (EC), raised speculations about unrecognized functions of GPIb-IX-V.[29-31] However, these data are not without controversy because others could not reproduce the findings.[32] No systematic investigations of GPIb-IX expression on a cellular level in situ have been performed to date.

As proposed recently,[33] the vWF-receptor complex may become an interesting pharmacologic target for the prevention of thrombotic and inflammatory complications. Because in vivo investigations are obviously limited in humans and nonhuman primates, there is a need for small animal models allowing for in vivo studies on GPIb-IX-V functions under normal and inflammatory conditions. In the mouse system, adequate animal models exist, but limited information about structure, function, and regulation of the murine receptor complex has been available. In the current study, we investigated the structural and functional proper-

From the Department of Molecular Oncology, General Surgery, University of Witten-Herdecke, and the BAYER Pharma Research Center, Wuppertal, Germany.

Submitted March 16, 1999; accepted September 20, 1999.

Supported by BAYER AG, Germany.

Reprints: Bernhard Nieswandt, IMMI, Klinikum Wuppertal, Universität Witten-Herdecke, Heusnerstrasse 40, D-42283 Wuppertal, Germany; e-mail: nieswand@klinikum-wuppertal.de.

The publication costs of this article were defrayed in part by page charge payment. Therefore, and solely to indicate this fact, this article is hereby marked ''advertisement'' in accordance with 18 U.S.C. section 1734.

© 2000 by The American Society of Hematology

Downloaded from http://ashpublications.net/blood/article-pdf/95/3/886/1660319/886.pdf by guest on 08 June 2024

ties of mouse GPIb-IX and examined the in vivo expression of the complex with novel monoclonal antibodies.

Materials and methods

Animals

Specific-pathogen-free mice (NMRI, BALB/c) 6 to 10 weeks of age were obtained from Charles River (Sulzfeld, Germany) and kept in our animal facilities.

Reagents

EZ-Link sulfo-NHS-LC-biotin (Pierce, Rockford, IL), immobilized pepsin (Pierce), ristocetin (EUROPA, Cambridge, UK), phorbol 12-myristate 13-acetate (PMA; Sigma, Deisenhofen, Germany), high molecular weight heparin (Sigma), thrombin (Boehringer Mannheim, Mannheim, Germany), Collagen A1 (Biochrom, Berlin, Germany), and streptavidin-horseradish peroxidase (HRP; DAKO, Glostrup, Denmark) were purchased. Lipopolysaccharide (LPS from *Salmonella minnesota* 9700) was obtained from Difco Laboratories (Detroit, Michigan).

Antibodies

Rat antimouse P-selectin mAb RB40.34 was kindly provided by D. Vestweber (Münster, Germany). Polyclonal rabbit antibodies to human fibrinogen and vWF were purchased from DAKO and were modified in our laboratories. Rabbit anti-fluorescein isothiocyanate (FITC)-HRP and rabbit anti-rat Ig-FITC were purchased from DAKO. All other antibodies were generated, produced, and modified in our laboratories: MWReg30 (anti-GPIIbIIIa, IgG1), JON1 (anti-GPIIbIIIa, IgG2b), EDL1 (anti-GPIIIa, IgG2a).

Platelet preparation and counting

Mice were bled under ether anesthesia from the retro-orbital plexus. Blood was collected in a tube containing 10% (vol/vol) 0.1 mol/L sodium citrate or 7.5 U/mL heparin, and platelet-rich plasma was obtained by centrifugation at 300*g* for 10 minutes at room temperature (RT). The platelets were washed twice with phosphate-buffered saline (PBS) by centrifugation at 1300*g* for 10 minutes and were used immediately. Isolated platelets did not show any signs of activation as shown by flow cytometry (staining for P-selectin and surface-expressed fibrinogen). For determination of platelet counts, blood (20 μL) was obtained from the retro-orbital plexus of anesthetized mice using siliconized microcapillaries and immediately diluted 1:100 in Unopette kits (Becton Dickinson, Heidelberg, Germany). The diluted blood sample was allowed to settle for 20 minutes in an Improved Neubauer Hemocytometer (Superior, Bad Mergentheim, Germany), and platelets were counted under a phase-contrast microscope at ×400 magnification.

Production of monoclonal antibodies

Female Wistar rats, 6 to 8 weeks of age, were immunized repeatedly with mouse platelets or with purified antigens. The rat spleen cells were then fused with mouse myeloma cells (Ag8.653), and hybridomas were selected in HAT medium. Hybridomas secreting mAbs directed against platelet receptors were identified by flow cytometry. Briefly, a 1:1 mixture of resting and thrombin-activated platelets (10^6) was incubated with 100 μL supernatant for 30 minutes at RT, washed with PBS (1300*g*, 10 minutes) and stained with FITC-labeled rabbit anti-rat Ig (DAKO) for 15 minutes. Samples were analyzed on a FACScan (Becton Dickinson) in the set-up mode. Platelets were gated by FSC/SSC-characteristics. Positive hybridomas were subcloned twice before large-scale production. Monoclonal antibodies were produced and purified according to standard methods. Isotype subclasses were determined by enzyme-linked immunosorbent assay (ELISA) with alkaline phosphatase (AP)-conjugated isotype-specific antibodies (Pharmingen): p0p 1, IgG2a; p0p 2, IgG1; p0p 3, IgG2a; p0p 4, IgG2b; p0p 5, IgG1.

Modification of antibodies

Affinity-purified antibodies were fluoresceinated to a fluorescein–protein ratio of approximately 3:1 by standard methods with FITC (Sigma) and separated from free FITC by gel filtration on a PD-10 column (Pharmacia, Uppsala, Sweden). HRP conjugation of mAbs was performed with a labeling kit (Boehringer Mannheim, Mannheim, Germany). $F(ab)_2$-fragments of p0p 3 and p0p 4 were generated by 24-hour incubation of 10 mg/mL mAb with immobilized pepsin (Pierce). Purity of the $F(ab)_2$-fragments was checked by sodium dodecyl sulphate–polyacrylamide gel electrophoresis (SDS-PAGE).

Immunoprecipitation and immunoblotting

Immunoprecipitation was performed as described previously.[34] Briefly, 10^8 washed platelets were surface labeled with EZ-Link sulfo-NHS-LC-biotin (Pierce; 100 μg/mL in PBS) and subsequently solubilized in 1 mL lysis buffer (Tris-buffered saline containing 20 mmol/L Tris/HCl, pH 8, 150 mmol/L NaCl, 1 mmol/L EDTA, 1 mmol/L phenylmethylsulfonyl fluoride, 2 μg/mL aprotinin, 0.5 μg/mL leupeptin, and 0.5% Nonidet P-40, all from Boehringer Mannheim). Cell debris was removed by centrifugation (15 000*g*, 10 minutes). After preclearing (8 hours), 10 μg mAb was added together with 25 μL protein G-Sepharose (Pharmacia), and precipitation took place overnight at 4°C. Samples were separated on 9% to 15% gradient SDS-PAGE along with a molecular weight marker and were transferred to a polyvinylidene difluoride (PVDF) membrane. The membrane was incubated with streptavidin-HRP (1 μg/mL) for 1 hour after blocking. After extensive washing, biotinylated proteins were visualized by echochemiluminescence (ECL; Amersham).

For immunoblotting, platelets were not surface labeled. After lysis, whole-cell extract was run on an SDS-PAGE gel and transferred to a PVDF membrane. The membrane was first incubated with 5 μg/mL FITC-labeled p0p 5 followed by rabbit anti-FITC-horseradish peroxidase (1 μg/mL). Proteins were visualized by ECL. Immunoprecipitation of GC from 1 mL of 1:10 diluted (PBS) mouse plasma was performed overnight at 4°C.

Flow cytometry

Freshly isolated platelets were washed twice with PBS and then resuspended in platelet buffer (20 mmol/L Tris HCl, pH 7, 0.9% NaCl, 1 mmol/L $CaCl_2$, and 1 mmol/L $MgCl_2$) at a concentration of 4×10^4/μL. Samples containing 25 μL of this dilution were stimulated with agonists for 10 minutes at RT, followed by the addition of saturating amounts of fluorophore-labeled antibodies or vice versa. After 15 minutes of incubation at RT, the samples were analyzed on a FACScan. PMA (50 ng/mL; Sigma) or thrombin (0.2 U/mL; Boehringer Mannheim) was used as agonists. For preincubation experiments, platelets were incubated with unlabeled mAbs for 15 minutes followed by the addition of saturating amounts of fluorophore-labeled antibodies. For analysis of ristocetin-induced platelet activation, platelets were incubated with 1.5 mg/mL ristocetin in the presence of 1 U/mL apyrase (grade III; Sigma) for 10 minutes at RT.

Immunohistochemistry

Acetone-fixed cryosections (6 μm) were blocked (5% normal goat serum, 5 mg/mL bovine serum albumin in PBS) for 30 minutes at RT. Primary mAbs were added at a final concentration of 2 μg/mL. After 90 minutes, the sections were washed 3 times with PBS and subsequently incubated with the adequate HRP-labeled secondary antibodies at a final concentration of 2 μg/mL for 60 minutes at RT. The AEC substrate was added after 3 washing steps, and the sections were then counterstained with hematoxylin.

Lipopolysaccharide treatment

Mice were injected with the indicated amounts of LPS (in 0.5 mL sterile PBS) intraperitoneally.

Sequencing

The antigen of 5×10^{10} unbiotinylated platelets was immunoprecipitated with p0p 3. After electrophoresis on SDS-PAGE and transfer to PVDF membrane, the

Downloaded from http://ashpublications.net/blood/article-pdf/95/3/886/1660319/886.pdf by guest on 08 June 2024

150-kd band was cut out and enzymatically deblocked with pyroglutamate aminopeptidase (sequencing grade; Boehringer Mannheim) as described.[35] The deblocked protein was subjected to an Applied Biosystems (Foster City, CA) protein sequencer (model 494) with an online PTH-analyzer.

Glycocalicin ELISA

Microtiter plates were coated with 15 μg/mL p0p 3 in coating buffer (50 mmol/L $NaHCO_3$, pH 9) overnight at 4°C. After blocking, serial dilutions of plasma or platelet supernatants were added to duplicate wells (1 hour, 37°C). Plates were washed and subsequently incubated with HRP-conjugated p0p 4 (5 μg/mL, 1 hour, 37°C). After extensive washing, TMB was added to each well, and the reaction was stopped by the addition of 2 N H_2SO_4 after 10 to 15 minutes. Absorbance at 450 nm was recorded on a Multiskan MCC/340 (Labsystems, Lugano, Switzerland).

Glycocalicin standard

The copy number of GPIbα on mouse platelets was estimated by flow cytometry by comparing Fl2 signals obtained with R-phycoerythrin (PE) conjugated p0p 3-5 on mouse platelets and a PE-conjugated antihuman GPIbα mAb on human platelets at identical instrument settings. The signal intensities obtained were in a similar range. Thus, the number of GPIbα molecules on human and mouse platelets was assumed to be similar (approximately 25 000). Washed platelets (5×10^8/mouse) from 10 healthy mice (5 NMRI, 5 Balb/c) were suspended in each 500 μL PBS (10^9 platelets/mL) and activated with PMA (50 ng/mL) for 20 minutes at RT. Efficiency of GC shedding in each sample was determined by flow cytometry (75.6% ± 3.4%). Platelets and debris were removed by centrifugation (15 000*g*, 15 minutes). The supernatants were tested in the GC-ELISA and were found to contain virtually identical amounts of GC. Based on the estimated copy number of 25 000/platelet GPIbα, it was calculated that approximately 18 750 GC molecules had been shed from each platelet. Therefore, the supernatants were assumed to contain approximately 1.875×10^{13} GC molecules per milliliter ($18\,750 \times 10^9$). Based on a molecular weight of 130 kd of GC, a GC concentration of 23.8 μg/mL in the pooled supernatants was calculated. The supernatant was diluted 1:100 in PBS, and aliquots were snap frozen in liquid nitrogen and stored at −70° C. Serial dilutions of this standard were used as a control of known GC concentration in each experiment. The GC concentration of the standard was defined as 1 arbitrary unit.

Results

p0p mAbs are directed against mouse GPIb-IX

A series of novel mAbs recognizing a highly expressed membrane glycoprotein complex on mouse platelets was generated. Five of these mAbs (p0p 1-5) were used to characterize the recognized antigen. As shown in Figure 1a, p0p 1-5 precipitated proteins of identical molecular weights (150 and 25 kd under reducing conditions) from resting surface-biotinylated mouse platelets. Although the 150-kd band was precipitated in comparable amounts by all mAbs, different quantities of the 25-kd chain were observed. We used p0p 5 for Western blot analysis of the immunoprecipitates, which demonstrated that the 150-kd proteins precipitated by the p0p mAbs were identical (Figure 1b). N-terminal amino acid sequencing of the enzymatically deblocked protein (see ''Materials and Methods'') identified the 150-kd protein as mouse GPIbα[36] [H(T)(X)(S)ISKVTSLLEV]. Flow cytometric experiments demonstrated that p0p 1-5 recognized nonoverlapping epitopes (not shown). GPIb and GPIIbIIIa are expressed in comparable amounts on the surface of resting mouse platelets as determined flow cytometrically by comparing fluorescence intensities obtained with the p0p mAbs and anti-GPIIbIIIa mAbs (JON1, MWReg30).

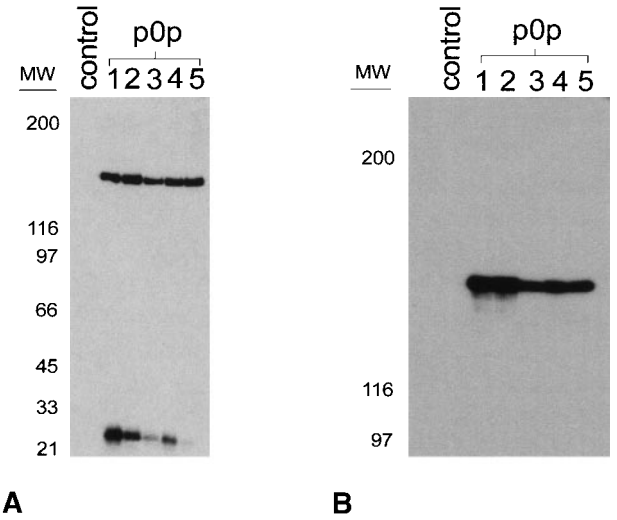

Figure 1. p0p mAbs are directed against mouse GPIb-IX. (A) Immunoprecipitation from surface-biotinylated resting platelets by p0p 1-5. NP-40 lysates were incubated with nonimmune rat IgG1 (control) or p0p 1-5, followed by protein G-Sepharose. Proteins were separated by 9% to 15% gradient SDS-PAGE under reducing conditions, transferred to a PVDF membrane, and detected by streptavidin-HRP and ECL. (B) Unlabeled platelet proteins were immunoprecipitated with nonimmune rat IgG1 (control) or p0p 1-5, followed by SDS-PAGE and immunoblotting with FITC-labeled p0p 5. Bound p0p 5 was detected by HRP-labeled rabbit anti-FITC.

Shedding of GPIbα is the dominant mechanism of GPIb-IX down-regulation on activation with thrombin or PMA

As shown in Figure 2a, activation of platelets with thrombin or PMA resulted in decreased binding of the p0p mAbs to the platelet surface, whereas signals for GPIIbIIIa (JON1) and P-selectin (not shown) significantly increased. Although staining with p0p 3-5 was almost completely abolished on activation, p0p 1,2 signals were just slightly decreased. To discriminate between receptor internalization and proteolytic cleavage, platelets were first incubated with fluorophore-labeled mAbs and activated with thrombin or PMA after 15 minutes (Figure 2b). Again, the results obtained with p0p 1,2 differed significantly from those obtained with p0p 3-5. Fl1 intensities of p0p 1,2 were virtually unaffected by both forms of activation under these conditions, indicating that the respective epitopes had been internalized. In contrast, fluorescence signals of p0p 3-5 decreased significantly on activation with thrombin or PMA, suggesting that the epitopes recognized by these mAbs had been cleaved from the platelet surface to approximately 47% and 75%, respectively. Immunoprecipitation studies demonstrated that p0p 3-5 recognized a soluble 130-kd fragment of the receptor (GC) in the supernatant of platelets activated with PMA (Figure 2c) or thrombin (not shown), whereas p0p 1,2 and control IgG1 did not. We concluded that p0p 1,2 either bound to GPIX or epitopes on GPIbα/β distinct from the GC portion. We were unable to localize the binding epitopes of p0p 1,2 on either GPIX, GPIbα, or GPIbβ because separation of the peptide chains by different approaches always abrogated binding of the mAbs. However, because binding of p0p 1,2 was unaffected by proteolytic cleavage of GPIbα, we expected these 2 mAbs to precipitate the truncated rest of this polypeptide chain (t-GPIbα) retained in the membrane after GC shedding (approximately 20 kd). Because this fragment is disulfide linked to GPIbβ (25 kd), an approximately 45-kd band had to be detectable under nonreducing conditions. Both the 20-kd band (red.) and the 45-kd band (nonred) were identified in the immunoprecipitates of p0p 1,2 but not of p0p 3 (Figure 2d) or p0p 4,5 (not shown).

Downloaded from http://ashpublications.net/blood/article-pdf/95/3/886/1660319/886.pdf by guest on 08 June 2024

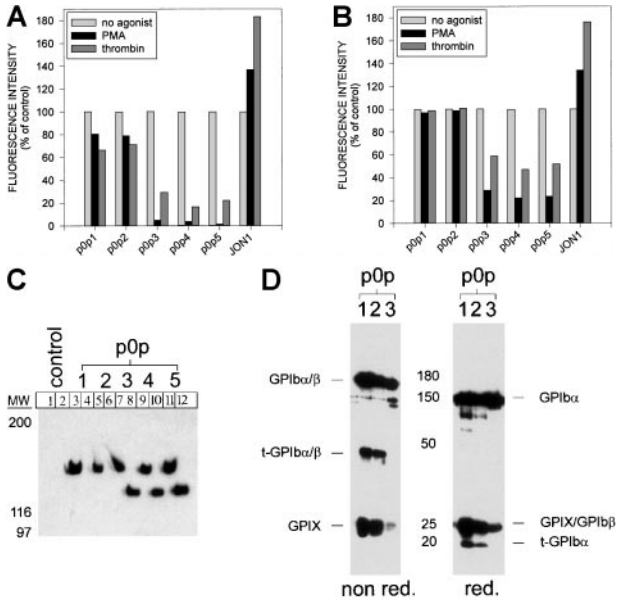

Figure 2. Effect of α-thrombin and PMA on p0p 1-5 binding to mouse platelets. Platelets were first incubated with 0.2 U/mL α-thrombin or 50 ng/mL PMA for 10 minutes at RT and subsequently stained with FITC-labeled mAbs for 15 minutes at RT (A) or vice versa (B). Samples were analyzed on a FACScan. The results shown are representative of 6 individual experiments. (C) Immunoprecipitation with p0p 1-5 and control IgG1 from NP-40 lysates of surface-biotinylated resting platelets (lanes 1, 3, 5, 7, 9, 11) or supernatant of PMA-activated surface-biotinylated platelets (lanes 2, 4, 6, 8, 10, 12; 10 minutes, at 15 000*g*). Proteins were separated by 9% to 15% SDS-PAGE under reducing conditions, transferred to a PVDF-membrane, and detected by streptavidin-HRP/ECL. (D) Detection of GPIbβ and the membrane-anchored truncated 20-kd remainder of GPIbα (t-GPIbα). Surface-biotinylated platelets were stimulated with PMA (50 ng/mL) for 10 minutes at RT, washed twice, and lysed with NP-40. Immunoprecipitates of p0p 1, p0p 2, and p0p 3 (control) were separated under reducing and nonreducing conditions and blotted onto a PVDF-membrane, and biotinylated proteins were detected by streptavidin-HRP/ECL.

Mouse plasma contains approximately 25 μg/mL glycocalicin

We performed immunoprecipitation with p0p 1-5 and JON1 (control) from normal mouse plasma and tested the immunoprecipitates for the presence of GC by Western blot analysis with p0p 5. As shown in Figure 3a, p0p 3-5, but not p0p 1,2 or JON1, had precipitated significant amounts of GC. For better quantification of GC in mouse plasma, we established an ELISA system using p0p 3 as capture and HRP-conjugated p0p 4 as detection antibody. Serial dilutions of supernatants from activated (PMA or thrombin) or resting platelets, normal mouse plasma, and a standard of known GC concentration (''Material and methods'') were tested (Figure 3b). Results showed that normal mouse plasma contains approximately 25 μg/mL GC and that a similar amount was shed from 10^9/mL PMA-activated platelets (physiological count). Therefore, the platelet-GPIbα:plasma GC ratio is approximately 1:1 in mouse blood, which was confirmed by a 2-fold increase of GC in platelet-rich plasma on PMA-induced activation. Plasma GC concentrations did not differ significantly between individual mice tested (± 5.8%; n = 30; different mouse strains).

Mouse GPIbα contains 3 different cleavage sites for platelet-derived proteases

Flow cytometric studies demonstrated that incubation of washed mouse platelets at RT resulted in time-dependent proteolytic degradation of GPIbα. Binding of p0p 1,2 remained virtually unaffected for 6 hours, whereas the epitopes recognized by p0p 5 and, to a greater extent p0p 3,4, were down-regulated, indicating progressive shedding of GPIbα rather than internalization of the receptor complex (not shown). We took advantage of this observation, incubated freshly isolated surface-biotinylated platelets for 6 hours at RT, and subsequently generated an NP-40 lysate containing the solubilized membrane proteins and all proteolytically cleaved fragments and release products. This lysate was used for immunoprecipitation with the p0p mAbs. Three different band patterns were found on the blot (Figure 4). p0p 1 (lane 2) and p0p 2 (not shown) had precipitated identical bands. Based on these results, we were able to identify 3 different cleavage sites on GPIbα, defining fragment pairs of 20 + 130 kd, 90 + 60 kd, and 105 + 45 kd, respectively. p0p 3,4 precipitated the 45-kd band (fragment 1a), whereas p0p 1, 5 precipitated the 105-kd band (fragment 1b). Based on the finding that p0p 1 precipitates the membrane-anchored fragment (see Figure 2d), we concluded that fragment 1a represents the cleaved N-terminal 45-kd fragment of GPIbα, whereas fragment 1b is the truncated 105-kd remainder of GPIbα retained in the membrane. Therefore, the binding epitopes of p0p 3,4 are located on the N-terminal 45-kd portion of the receptor known to contain the binding sites for vWF and thrombin.[7-9] Furthermore, p0p 3-5 precipitated the 60-kd band (fragment 2a), whereas the 90-kd band (fragment 2b) was exclusively recognized by p0p 1 (and p0p 2). The latter therefore represented the membrane-anchored truncated remainder of GPIbα. We concluded that p0p 5 binds to an epitope on the N-terminal 60-kd portion of GPIbα located between cleavage sites 1 and 2. The 130-kd band (fragment 3a), recognized by p0p 3-5, was identified as GC, whereas the 20-kd band (fragment 3b) exclusively recognized by p0p 1,2 represented the corresponding membrane-anchored truncated form of GPIbα (t-GPIbα).

Occupancy of GPIbα induces irreversible aggregate formation in vitro and rapid thrombocytopenia in vivo

Standard aggregometry demonstrated that none of the p0p mAbs (at concentrations of 10, 30, or 100 μg/mL) interfered with aggregation induced by adenosine diphosphate, collagen, PMA, or ristocetin (not shown). We observed, however, that ristocetin (at concentrations greater than 1 mg/mL) did not induce passive

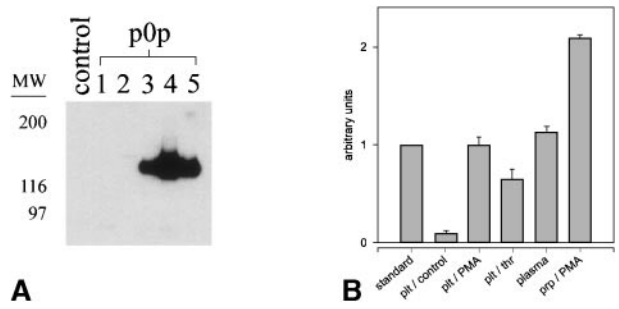

Figure 3. Detection and quantification of glycocalicin in mouse plasma. Blood (50 μL) was collected in 200 μL heparinized PBS and diluted 1:10 with PBS. Cells and microparticles were removed by centrifugation. (A) Immunoprecipitation from normal mouse plasma with p0p 1-5 and a nonimmune IgG1 (control), followed by immunoblotting with p0p 5-FITC. Bound p0p 5 was detected by HRP-labeled rabbit anti-FITC/ECL. (B) Detection and quantification of glycocalicin in mouse plasma and the supernatants of mouse platelets using a sandwich-type ELISA (p0p 3,4-HRP). Washed platelets (10^9/mL) or platelet-rich plasma were activated with either PMA (50 ng/mL) or thrombin (thr; 0.2 U/mL) or were incubated without agonist (control) for 15 minutes at RT. Supernatants were prepared by centrifugation at 15,000*g* for 10 minutes and were tested along with normal mouse plasma and a standard of known GC concentration (23.8 μg/mL) in serial dilutions. See "Materials and methods" for details.

Downloaded from http://ashpublications.net/blood/article-pdf/95/3/886/1660319/886.pdf by guest on 08 June 2024

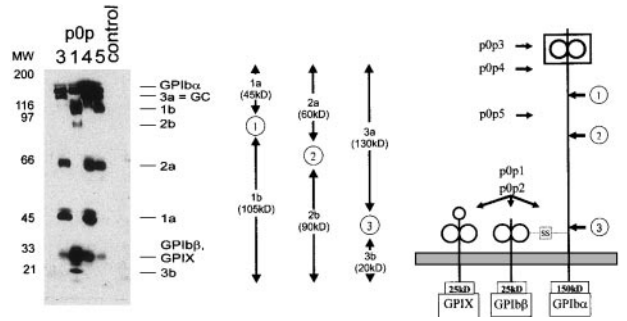

Figure 4. Immunoprecipitation of 6 different proteolytic fragments of GPIbα. Surface-biotinylated mouse platelets were incubated for 6 hours at RT and lysed directly. Immunoprecipitation was performed with p0p 1,3,4,5 and control IgG1. Proteins were separated by 9% to 15% SDS-PAGE under reducing conditions and were detected by streptavidin-HRP/ECL. (right) Schematic drawing of the murine GPIb-IX complex. (arrows) Proposed cleavage sites (1, 2, 3). (left, arrows) Assumed binding sites of p0p 1-5. (middle) Schematic drawing of fragment pairs shown on the blot.

agglutination (as described for human platelets) but did induce active aggregation of mouse platelets as evidenced by rapid surface expression of P-selectin, fibrinogen, and vWF in the presence of this antibiotic (Figure 5).

Although no inhibitory effect of the p0p mAbs on platelet aggregation could be detected, direct platelet activation by all mAbs directed against the GC portion of GPIbα was obvious. Addition of (10-100 μg/mL) p0p 3-5 or $F(ab)_2$-fragments of p0p 3,4, but not p0p 1,2 or control IgG, to platelet-rich plasma under stirring conditions (1000 rpm, 37°C) induced the formation of microaggregates of 3 to 5 platelets (not shown). Platelet activation induced by p0p 3-5 became more evident after mild centrifugation of the samples (1300*g*, 5 minutes, RT).

After resuspension, large aggregates were found, whereas the single platelet count was drastically reduced (Figure 6a). Flow cytometric analysis of the aggregates demonstrated no increased surface expression of P-selectin, vWF, or fibrinogen (not shown). In correlation with platelet aggregating effects in vitro, we found rapid and irreversible platelet depletion on the injection of 25 μg per mouse p0p 3-5 or $F(ab)_2$-fragments of p0p 3,4, whereas thrombocytopenia induced by p0p 1,2 or EDL1 (anti-gpIIIa) was less effective (Figure 6b).

GPIb-IX is not detectable on endothelial cells under normal or inflammatory conditions

To examine the in vivo protein expression of GPIb-IX, cryosections from the major organs (spleen, lung, liver, kidney, heart, brain, intestine, skin, and thymus) from normal mice (n = 6) were stained for GPIb-IX with a 1:1 mixture of p0p 1 and p0p 4 (each at 2 μg/mL). Antibodies against vWf were used as a control for staining the platelets, megakaryocytes, and endothelial cells.

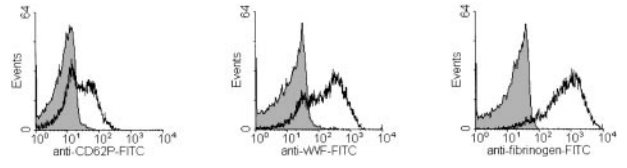

Figure 5. Ristocetin induces activation of mouse platelets. Platelets (10^6) were incubated with 1.5 mg/mL ristocetin in the presence of 1 U/mL apyrase at RT for 10 minutes. Subsequently, FITC-labeled antibodies were added in saturating amounts, and the samples were analyzed on a FACScan after 15 minutes. (shaded area) Staining of resting platelets. (solid lines) Staining of ristocetin-activated platelets.

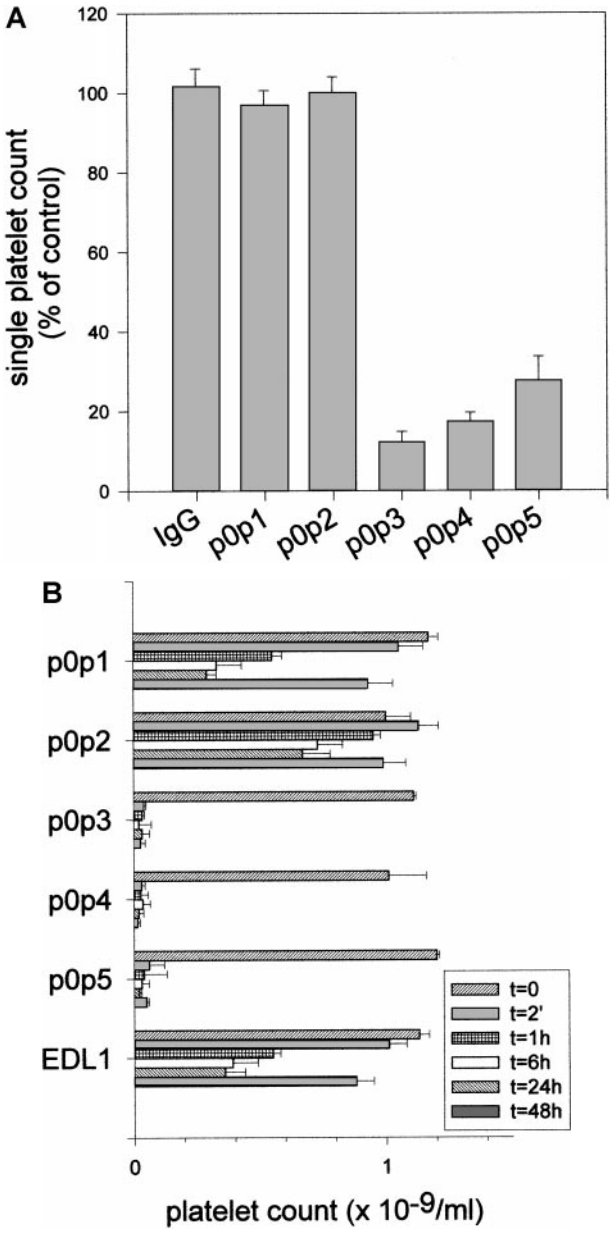

Figure 6. p0p 3-5 induce aggregate formation in vitro and rapid thrombocytopenia in vivo. (A) Washed platelets (2×10^6) were incubated with 10 mg/mL of the indicated mAbs or without antibody (control) for 15 minutes at RT, followed by centrifugation at 1300*g* for 5 minutes. After resuspension of the pellets by vortexing for 5 seconds, the single platelet count in the samples was determined by flow cytometry. Results are shown as the mean ± SD for 3 independent experiments. (B) Normal female NMRI mice received 25 μg purified p0p 1,2,5 or $F(ab)_2$-fragments of p0p 3,4 intravenously in 200 μL sterile PBS. The anti-GPIIIa mAb EDL1 was used as a control. Platelet counts were determined at the indicated times using an Improved Neubauer hemocytometer. Injection of a nonimmune IgG1 had no significant effect on the platelet count (not shown). Intact p0p 3,4 induced comparable thrombocytopenia as the $F(ab)_2$-fragments (not shown). Results of platelet count are shown as the mean ± SD for groups of 3 mice. The experiment was repeated twice with comparable results.

p0p1,4, and anti-vWF specifically stained megakaryocytes and platelets in the red pulp of the spleen (Figure 7). In the lungs, only platelets but not endothelial or other cells were stained with p0p 1 and p0p 4, whereas anti-vWF stained platelets and endothelial cells. In the liver, kidney, and heart, few platelets were detectable with p0p 1, p0p 4, and anti-vWF. As in the lungs, specific staining

Downloaded from http://ashpublications.net/blood/article-pdf/95/3/886/1660319/886.pdf by guest on 08 June 2024

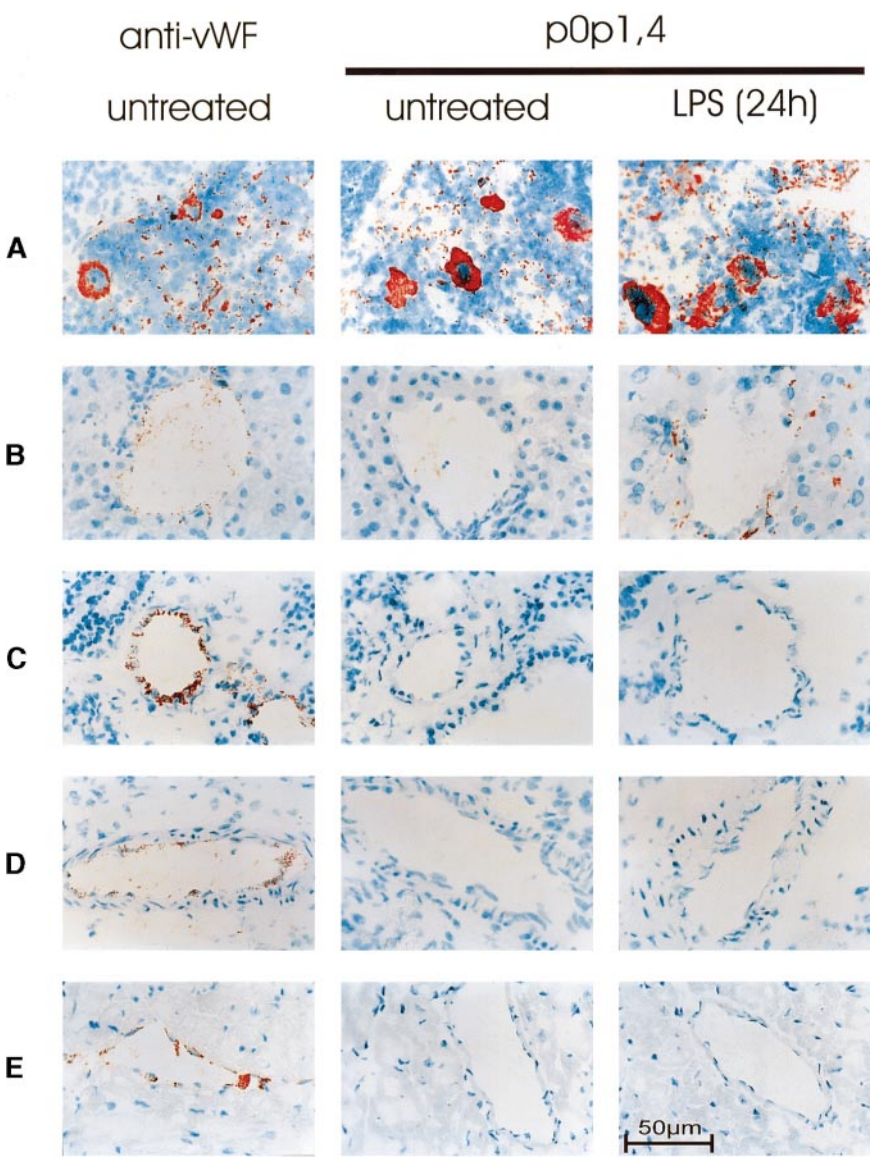

Figure 7. Immunohistochemical detection of GPIb-IX. Acetone-fixed frozen sections from normal (untreated) mice and mice 24 hours after injection of 20 mg/kg LPS were stained for GPIb-IX with p0p 1,4. As a positive control for platelet/megakaryocytic and endothelial expression, sections from normal mice were stained for vWF (left). Representative sections of (A) spleen, (B) liver, (C) lung, (D) kidney, and (E) heart are shown.

of endothelial cells was only detectable with anti-vWF. The same result was obtained with brain, intestine, skin, and thymus (not shown), in which virtually no platelets were detected. The staining pattern obtained with p0p 1, p0p 4, and JON1 (anti-GPIIbIIIa, not shown) was identical in all organs examined. Thus, no expression of GPIb-X on cells other than platelets/megakaryocytes was detectable in any organ of normal healthy mice. To test the hypothesis that GPIb-IX might be expressed on endothelial cells in response to inflammatory stimuli,[10,29,30] we treated mice with bacterial LPS (20 mg/kg, n = 20). It is well documented that such treatment induces the production of a variety of cytokines, resulting in systemic inflammatory responses in mice.[37] Significant thrombocytopenia (platelet count, 61.4% ± 4.9% of normal) and hypothermia (−3.3°C ± 0.6°C) developed in all mice within 12 hours. Organs from 5 mice were sampled after 6, 12, 24, or 48 hours, and cryosections were stained with p0p 1, p0p 4, anti-vWF, or JON1. Although all antibodies stained platelets and megakaryocytes, specific staining of endothelial cells in these organs was only observed with anti-vWF. A significantly increased number of platelets in the livers of LPS-treated mice was detected with p0p 1 and p0p 4 (and JON1), whereas staining of platelets in the lungs and platelets/megakaryocytes in the spleens was apparently unchanged compared with that in the control mice. As in the control mice, kidney, heart, skin, intestine, brain, and thymus appeared virtually free of platelets (the latter 4 organs are not shown).

Discussion

In the current study we investigated the structural and functional properties of mouse GPIb-IX and systematically examined the in vivo expression of the receptor on a cellular level for the first time. For our studies we used 5 newly developed monoclonal antibodies that recognized different, nonoverlapping epitopes on the complex. Immunoprecipitation and Western blot analysis showed that the individual components of the complex had apparent molecular weights similar to those of human homologs: GPIbα (approximately 150 kd), GPIbβ (approximately 25 kd), and GPIX (approximately 25 kd) (Figures 1, 2). Using p0p 1-5 for flow cytometric and biochemical analyses, we were able to examine and quantify the regulation of different epitopes on mouse GPIb-IX under various experimental conditions. In our experiments, we found that throm-

Downloaded from http://ashpublications.net/blood/article-pdf/95/3/886/1660319/886.pdf by guest on 08 June 2024

bin-induced activation of mouse platelets resulted in approximately 47% shedding of GPIbα (GC) and only approximately 31% internalization of the GPIb-IX complex. In contrast, thrombin has been reported to induce internalization of GPIb-IX complexes from the platelet surface to the surface-connected canalicular system without evidence for receptor shedding on human platelets,[20-22] though this finding is not commonly accepted.[23,24] Therefore, it seems likely that mouse GPIbα is more susceptible to proteolytic cleavage during platelet activation. This hypothesis may be supported by the detection of at least 10-fold higher GC concentrations in mouse plasma than in human plasma (approximately 25 μg/mL versus approximately 2 μg/mL[38]). Certainly, the higher platelet counts in mice (1.0-1.2 $\times$ 10^6/μL versus 0.2-0.4 $\times$ 10^6/μL) also contribute to the marked difference in plasma GC concentrations between the 2 species.

Although GC is the only known fragment of human GPIbα generated by platelet-derived proteases, an additional N-terminal 45-kd fragment can be generated experimentally by trypsin digestion.[8] This 45-kd fragment, isolated by tryptic digestion or expressed by recombinant DNA methods, contains the binding sites for vWF and thrombin and essentially mimics the functional properties of GPIb-IX-V as a soluble receptor.[7-9] In our immunoprecipitation experiments with washed platelets, we identified 3 different soluble fragments (GC, 60 kd and 45 kd) and the 3 corresponding membrane-anchored truncated forms of GPIbα (20 kd, 90 kd, and 105 kd), demonstrating that these fragments must have been generated by platelet-derived proteases (Figure 4). To our knowledge, this is the first report describing the proteolytic generation of both the 45-kd and the 60-kd N-terminal fragment of GPIbα by platelet-derived proteases. Based on our data, we propose 3 cleavage sites on murine GPIbα (Figure 4), suggesting complex regulation mechanisms of GPIb-IX function in vivo. In contrast, in vitro activation of platelets with thrombin or PMA only resulted in proteolytic generation of GC but not of the 45-kd and 60-kd fragments of GPIbα (not shown). Most information on GPIb-IX-V regulation in humans is derived from studies using exogenous platelet-activating stimuli. This may explain why GC is the only known proteolytic fragment of GPIbα cleaved from activated human platelets.

The GPIbα–vWF interaction has become a potentially interesting target for antithrombotic therapies,[39] leading to the development of strategies for receptor or ligand blockage in vivo. Although mAbs against the A1-domain of vWF efficiently blocked GPIbα–vWF interaction in vivo,[39] there are conflicting reports about the in vivo effects of anti–GPIbα mAbs. Becker et al[40] reported that $F(ab)_2$-fragments of an anti-GPIbα mAb inhibited GPIb–vWF interactions in vivo and ex vivo without significant effects on platelet counts in guinea pigs. In contrast, a more recent study performed in baboons showed that the injection of anti–GPIbα-$F(ab)_2$-fragments immediately resulted in profound irreversible thrombocytopenia.[41] We observed similar effects in the mouse. All mAbs or $F(ab)_2$-fragments against the GC portion of GPIbα, irrespective of their exact binding epitope, induced aggregate formation in vitro and a greater than 95% drop of platelet count within 2 minutes in vivo (Figure 6). Although the mechanisms underlying this cytotoxic effect could not be identified in the current study, it seems possible that attempts to block certain epitopes on GPIb with modified antibodies in vivo may generally result in thrombocytopenia. In contrast to the inhibition of GPIIbIIIa function,[42] in vivo blockage of certain epitopes on GPIb may, therefore, not be a promising antithrombotic strategy.

Monoclonal antibodies directed against human GPIbα have been reported to inhibit ristocetin-induced platelet agglutination and to interfere with collagen-induced platelet aggregation.[43] Our aggregometric studies with p0p 1-5, however, showed that none of the mAbs had significant influence on aggregation induced by adenosine diphosphate, collagen, and PMA (not shown). Furthermore, p0p 1-5 had no effect on ristocetin-induced platelet aggregation, which was always associated with classical platelet activation. Concentrations greater than 1 mg/mL ristocetin induced surface expression of P-selectin, fibrinogen, and endogenous vWF, as determined by flow cytometry (Figure 5). The direct activation of mouse platelets by ristocetin contrasts its passive agglutination of human platelets.[14] Thus, ristocetin may not be suited for studies on GPIbα–vWF interactions in the mouse system.

The expression of GPIb-IX on cells of nonmegakaryocytic origin (particularly endothelial cells) has been controversial. Although the importance of the complex in normal megakaryocyte and platelet physiology is clear and well documented, some authors have speculated on a second, unrelated role of GPIb or the GPIb-IX-V complex.[29-31] This hypothesis is based on the observation that cultured human endothelial and smooth muscle cells express the individual subunits of the complex.[31,44-46] Furthermore, endothelial GPIbα has been proposed to be involved in platelet–endothelial cell interactions under inflammatory conditions.[29,30,47] On the other hand, these data are not without debate because the findings could not be reproduced by others.[32] Recently, Fujita et al[48] made the first attempt to examine the in vivo expression of GPIbα in the mouse. The authors reported consistent and reproducible GPIbα gene activity in nonhematopoietic organs, including lung and heart, and they speculated on GPIbα expression on cells other than platelets/megakaryocytes. Although GPIb-IX-V can be detected immunohistochemically on cultured human endothelial cells,[29-31] no systematic studies on the in vivo expression of the receptor on a cellular level have been performed to date. We examined GPIb-IX expression under normal and inflammatory conditions immunohistochemically for the first time and found specific staining in the major organs of the mouse only on platelets and megakaryocytes, but not on endothelial cells (Figure 7). Comparison between JON1 (anti-GPIIbIIIa) and p0p 1,4 (anti–GPIb-IX)-stained sections demonstrated identical staining patterns in all organs examined. In contrast, antibodies against vWF clearly stained platelets/megakaryocytes and endothelial cells. Although the sensitivity of immunohistochemical techniques is limited, our studies did not support the hypothesis that GPIb-IX is expressed on endothelial cells in vivo.

In conclusion, the results presented in this article indicate that mouse GPIb-IX was exclusively expressed on platelets and megakaryocytes and, despite some differences, shared many structural and functional properties with the human receptor. The p0p mAbs proved powerful tools, and they may be helpful for further studies on the function and regulation of the GPIb-IX complex. The availability of transgenic and knockout strains predestinates the mouse system for such investigations.

Acknowledgments

We thank N. Huss for critically reading the manuscript, E. Rieke for assisting with photography and computer data, and W. Heil for permission to use his aggregometer and chemicals. We also thank R. Müller-Peddinghaus, P. G. Höher, and J. Werner for their support throughout the study.

Downloaded from http://ashpublications.net/blood/article-pdf/95/3/886/1660319/886.pdf by guest on 08 June 2024

References

1. Nurden AT, Caen JP. Specific roles for platelet surface glycoproteins in platelet function. Nature. 1975;255:720.
2. Caen JP, Nurden AT, Jeanneau C, et al. Bernard-Soulier syndrome: a new platelet glycoprotein abnormality: its relationship with platelet adhesion to subendothelium and with the factor VIII von Willebrand protein. J Lab Clin Med. 1976;87:586.
3. Lopez JA. The platelet glycoprotein Ib-IX complex. Blood Coagul Fibrinolysis. 1994;5:97.
4. Savage B, Saldivar E, Ruggeri ZM. Initiation of platelet adhesion by arrest onto fibrinogen or translocation on von Willebrand factor. Cell. 1996; 84:289.
5. Lopez JA, Leung B, Reynolds CC, Li CQ, Fox JE. Efficient plasma membrane expression of a functional platelet glycoprotein Ib-IX complex requires the presence of its three subunits. J Biol Chem. 1992;267:12,851.
6. Modderman PW, Admiraal LG, Sonnenberg A, von dem Borne AE. Glycoproteins V and Ib-IX form a noncovalent complex in the platelet membrane. J Biol Chem. 1992;267:364.
7. Jandrot-Perrus M, Bouton MC, Lanza F, Guillin MC. Thrombin interaction with platelet membrane glycoprotein Ib. Semin Thromb Hemost. 1996;22:151.
8. Murata M, Ware J, Ruggeri ZM. Site-directed mutagenesis of a soluble recombinant fragment of platelet glycoprotein Ib alpha demonstrating negatively charged residues involved in von Willebrand factor binding. J Biol Chem. 1991;266: 15,474.
9. Vicente V, Kostel PJ, Ruggeri ZM. Isolation and functional characterization of the von Willebrand factor-binding domain located between residues His1-Arg293 of the alpha-chain of glycoprotein Ib. J Biol Chem. 1988;263:18,473.
10. George JN, Nurden AT, Phillips DR. Molecular defects in interactions of platelets with the vessel wall. N Engl J Med. 1984;311:1084.
11. Loscalzo J, Inbal A, Handin RI. von Willebrand protein facilitates platelet incorporation in polymerizing fibrin. J Clin Invest. 1986;78:1112.
12. Lankhof H, Wu YP, Vink T, et al. Role of the glycoprotein Ib-binding A1 repeat and the RGD sequence in platelet adhesion to human recombinant von Willebrand factor. Blood. 1995;86:1035.
13. Ikeda Y, Handa M, Kawano K, et al. The role of von Willebrand factor and fibrinogen in platelet aggregation under varying shear stress. J Clin Invest. 1991;87:1234.
14. Coller BS, Gralnick HR. Studies on the mechanism of ristocetin-induced platelet agglutination: effects of structural modification of ristocetin and vancomycin. J Clin Invest. 1977;60:302.
15. Read MS, Smith SV, Lamb MA, Brinkhous KM. Role of botrocetin in platelet agglutination: formation of an activated complex of botrocetin and von Willebrand factor. Blood. 1989;74:1031.
16. Hoylaerts MF. Platelet-vessel wall interactions in thrombosis and restenosis role of von Willebrand factor. Verh K Acad Geneeskd Belg. 1997;59:161.
17. Shattil SJ, Ginsberg MH, Brugge JS. Adhesive signaling in platelets. Curr Opin Cell Biol. 1994;6:695.
18. Fujimoto T, Hawiger J. Adenosine diphosphate induces binding of von Willebrand factor to human platelets. Nature. 1982;297:154.
19. Gralnick HR, Williams SB, Coller BS. Fibrinogen competes with von Willebrand factor for binding to the glycoprotein IIb/IIIa complex when platelets are stimulated with thrombin. Blood. 1984;64:797.
20. Nurden A, Cazes E, Bihour C, et al. Confirmation that GP Ib-IX complexes have a reduced surface distribution on platelets activated by thrombin and TRAP-14-mer peptide. Br J Haematol. 1995; 90:645.
21. Lu H, Menashi S, Garcia I, et al. Reversibility of thrombin-induced decrease in platelet glycoprotein Ib function [see comments]. Br J Haematol. 1993;85:116.
22. Michelson AD, Benoit SE, Kroll MH, et al. The activation-induced decrease in the platelet surface expression of the glycoprotein Ib-IX complex is reversible. Blood. 1994;83:3562.
23. Fox JE. Shedding of adhesion receptors from the surface of activated platelets. Blood Coagul Fibrinolysis. 1994;5:291.
24. White JG, Escolar G. Fate of the GPIb/IX receptor complex following activation of human platelets. Blood Coagul Fibrinolysis. 1996;7:262.
25. LaRosa CA, Rohrer MJ, Benoit SE, Barnard MR, Michelson AD. Neutrophil cathepsin G modulates the platelet surface expression of the glycoprotein (GP) Ib-IX complex by proteolysis of the von Willebrand factor binding site on GPIb alpha and by a cytoskeletal-mediated redistribution of the remainder of the complex. Blood. 1994;84:158.
26. Wicki AN, Clemetson KJ. Structure and function of platelet membrane glycoproteins Ib and V: effects of leukocyte elastase and other proteases on platelets response to von Willebrand factor and thrombin. Eur J Biochem. 1985;153:1.
27. Michelson AD, Loscalzo J, Melnick B, Coller BS, Handin RI. Partial characterization of a binding site for von Willebrand factor on glycocalicin. Blood. 1986;67:19.
28. Nurden AT. Congenital abnormalities of platelet membrane glycoproteins. In: Kunicki TJ, George JN, eds. Platelet Immunobiology. Philadelphia: JB Lippincott; 1989:63.
29. Konkle BA, Shapiro SS, Asch AS, Nachman RL-.Cytokine-enhanced expression of glycoprotein Ib alpha in human endothelium. J Biol Chem. 1990; 265:19,833.
30. Rajagopalan V, Essex DW, Shapiro SS, Konkle BA. Tumor necrosis factor-alpha modulation of glycoprotein Ib alpha expression in human endothelial and erythroleukemia cells. Blood. 1992;80:153.
31. Wu G, Essex DW, Meloni FJ, et al. Human endothelial cells in culture and in vivo express on their surface all four components of the glycoprotein Ib/IX/V complex. Blood. 1997;90:2660.
32. Perrault C, Lankhof H, Pidard D, et al. Relative importance of the glycoprotein Ib-binding domain and the RGD sequence of von Willebrand factor for its interaction with endothelial cells. Blood. 1997;90:2335.
33. Goto S, Ikeda Y, Saldivar E, Ruggeri ZM. Distinct mechanisms of platelet aggregation as a consequence of different shearing flow conditions. J Clin Invest. 1998;101:479.
34. Rehli M, Krause SW, Kreutz M, Andreesen R. Carboxypeptidase M is identical to the MAX. 1 antigen and its expression is associated with monocyte to macrophage differentiation. J Biol Chem. 1995;270:15,644.
35. Hirano T, Komatsu S, Tsunasawa H. Protein sequencing protocols. In: Smith BJ eds. Totowa, NJ: Human Press; 1997:287.
36. Ware J, Russell S, Ruggeri ZM. Cloning of the murine platelet glycoprotein Ibα gene highlighting species-specific platelet adhesion. Blood Cells Mol Dis. 1997;23:292.
37. McCuskey RS, Urbaschek R, Urbaschek B. The microcirculation during endotoxemia. Cardiovasc Res. 1996;32:752.
38. Beer JH, Buchi L, Steiner B. Glycocalicin: a new assay—the normal plasma levels and its potential usefulness in selected diseases. Blood. 1994;83:691.
39. Kageyama S, Yamamoto H, Nagano M, Arisaka H, Kayahara T, Yoshimoto R. Anti-thrombotic effects and bleeding risk of AJvW-2, a monoclonal antibody against human von Willebrand factor. Br J Pharmacol. 1997;122:165.
40. Becker BH, Miller JL: Effects of an antiplatelet glycoprotein Ib antibody on hemostatic function in the guinea pig. Blood. 1989;74:690.
41. Cadroy Y, Hanson SR, Kelly AB, et al. Relative antithrombotic effects of monoclonal antibodies targeting different platelet glycoprotein-adhesive molecule interactions in nonhuman primates. Blood. 1994;83:3218.
42. Topol EJ, Byzova TV, Plow EF. Platelet GPIIb-IIIa blockers. Lancet. 1999;353:227.
43. Frojmovic MM. Platelet aggregation in flow: differential roles for adhesive receptors and ligands. Am Heart J. 1999;135(suppl):S119.
44. Asch AS, Adelman B, Fujimoto M, Nachman RL. Identification and isolation of a platelet GPIb-like protein in human umbilical vein endothelial cells and bovine aortic smooth muscle cells. J Clin Invest. 1988;81:1600.
45. Kelly MD, Essex DW, Shapiro SS, et al. Complementary DNA cloning of the alternatively expressed endothelial cell glycoprotein Ib beta (GPIb beta) and localization of the GPIb beta gene to chromosome 22 [see comments]. J Clin Invest. 1994;93:2417.
46. Beacham DA, Tran LP, Shapiro SS. Cytokine treatment of endothelial cells increases glycoprotein Ib alpha-dependent adhesion to von Willebrand factor. Blood. 1997;89:4071.
47. Bombeli T, Schwartz BR, Harlan JM. Adhesion of activated platelets to endothelial cells: evidence for a GPIIbIIIa-dependent bridging mechanism and novel roles for endothelial intercellular adhesion molecule 1 (ICAM-1), alphavbeta3 integrin, and GPIbalpha. J Exp Med. 1998;187:329.
48. Fujita H, Hashimoto Y, Russell S, Zieger B, Ware J. In vivo expression of murine platelet glycoprotein Ibalpha. Blood. 1998;92:488.

Downloaded from http://ashpublications.net/blood/article-pdf/95/3/886/1660319/886.pdf by guest on 08 June 2024